

On-demand Wireless Infusion Rate Control in an Implantable Micropump for Patient-tailored Treatment of Chronic Conditions

Roya Sheybani-EMBS Student Member, and Ellis Meng, IEEE Senior Member

Abstract— Wireless infusion rate control and programmability for an implantable, low power, electrochemical micropump is presented. Flow rate control was achieved through adjustment of the wiper position of a current potentiometer in the wireless receiver (0.6-3.2 mA output current with a resolution of 0.2 mA per step). An off-the-shelf Bluetooth module and Basic Stamp microcontroller kit was used to initiate amplitude-shift keying (ASK) modulation of the inductive power signal. Accurate flow control of two model regimens was achieved on benchtop. Wireless transmission (power transfer and control) was not affected by simulated tissue material placed between the transmitter and receiver.

I. INTRODUCTION

Effective drug therapy is essential in the treatment and management of chronic conditions such as hypertension, respiratory disease, and diabetes [1]. As of 2005, 46% of American adults suffer from at least one chronic illness and 75% of health care dollars are spent on the treatment of chronic diseases [2]. Implantable drug delivery devices may improve treatment of chronic conditions by bypassing physiological barriers to enable delivery of new compounds such as biologics, biosimilars, and other small molecules directly to the target tissue [3]; and maximizing therapeutic efficacy of the drug and limiting toxic side effects by delivering the correct amount of drug in the vicinity of the target cells, while reducing the drug exposure to the non-target cells [4]. Most commercial implantable pumps only provide constant infusion rate. Certain chronic conditions, such as drug addiction and menopause, have associated static therapeutic windows and may be treated with continuous flow drug administration [5], however, many chronic conditions have chronobiological pattern in their pathogenesis [6-9]. More importantly, drug dosing affects the therapeutic window. Following successful drug administration, the clinical need for additional pharmacological intervention for certain conditions diminishes transiently while the ratio of risk to benefit dramatically increases [10]. Controlled patient-tailored drug administration avoids the peak and trough time course of drug concentrations in the plasma between successive doses and the corresponding peak and trough pattern of drug action, leading to therapies that mimic chronobiological patterns [3, 11, 12].

Implantable pumps are advantageous for chronic

treatment; eliminating transcutaneous wires and catheters permits improved patient mobility and allows drug administration outside of clinical settings [13]. Despite advances in miniaturization, batteries are still large in comparison to microelectromechanical systems (MEMS) pump actuators and can significantly increase device size. Also, batteries have limited lifetime and may pose health risks (leakage or malfunction) [14]. Wireless powering and control of drug delivery devices eliminates the battery, reduces device dimensions, and can improve system lifetime.

A wired programmable and implantable drug infusion micropump system, capable of delivering a diverse assortment of liquid drug formulations with high accuracy within a wide dynamic range of dose volumes and flow rates, as well as wireless powering at a single flow rate, were previously demonstrated by our group [15, 16]. Here, we present, for the first time, a completely wireless infusion micropump system with flow rate adjustability capable of achieving patient-tailored therapy. Our research prototype is currently scaled for small animal (rodents) research (Fig. 1). The animal with the implanted micropump system is placed inside a cage set atop the transmitting coil. The user-defined delivery parameters (duration and infusion rate) are entered on-demand or stored as a program on a laptop that communicates via Bluetooth with the transmitter circuit to control operation of the implanted pump.

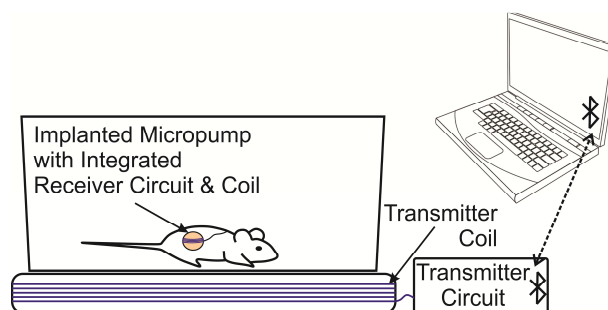


Figure 1: Schematic diagram of system setup for small animal research.

II. DESIGN AND FABRICATION

A. System Requirements

The micropump consists of an electrolysis driven actuator housed in a drug reservoir. Interdigitated Nafion[®]-coated platinum (Pt) electrodes electrolyze the water in the actuation chamber into hydrogen and oxygen upon electric current application. The resulting volume expansion is harnessed to inflate a Parylene bellows and expel fluid in the adjacent drug chamber through a catheter to the target site [16]. The current-controlled actuator requires 0.66-51.31 mW of power (for 0.1-13 mA applied current) to achieve a wide range of flow rates (0.33 - 141.9 μ L/min, respectively). Here, we limit

*Research supported in part by NSF through the PFI: AIR Technology Translation program (award number IIP-1343467) and NIH (award number R21GM104583) funding sources.

E. Meng, and R. Sheybani are with the Department of Biomedical Engineering, Viterbi School of Engineering, University of Southern California, Los Angeles, CA 90089-1111 USA (corresponding author: 213-821-3949, e-mail: ellis.meng@usc.edu).

the flow rate range to 2.0 - 25.0 $\mu\text{L}/\text{min}$ (0.6-3.2 mA applied current) which is suitable for most small animal research applications. The overall device footprint should also be minimized to allow for implantation in mice ($\varnothing < 22$ mm, height < 10 mm). Wireless inductive powering was chosen to satisfy the low power and small footprint requirements, as well to maximize the usable lifetime of the device.

Under constant current conditions, production and mass transfer of electrolysis gases is proportional to the square root of time [17-19]. Thus, constant current is the preferred mode for electrolysis actuation, producing an infusion rate linearly proportional to current. For a single infusion rate, the power received is rectified and applied to a current regulator to provide a single constant current to the actuator. Variable current (and therefore variable infusion rates) could be achieved by changing the wiper position of a current setting programmable digital potentiometer in the receiver circuit to alter the output current. The potentiometer should be chosen to allow for the selection of the full range of desired currents (0.6 -3.2 mA) with a resolution of 0.2 mA per step. The wiper position could be changed using a data signal wirelessly transferred through the skin to the receiver. Two methods of data transmission were considered for this purpose: infrared and ASK. ASK was chosen due to its simplicity, lower number of additional components on the transmitter and receiver circuits, and lower susceptibility to environmental noise.

B. System Architecture

Using the ASK data transmission method, a low frequency data signal is carried by the power signal and subsequently demodulated on the receiver. Pulse width of the data signal determines the number of incremental steps of potentiometer wiper position, altering the potentiometer resistance, and changing the output current set by the potentiometer. The transmitter output is controlled by the Easy Bluetooth module and Basic Stamp microcontroller kit (Parallax Inc., Rocklin, CA) and custom user interface program using the Basic Stamp editor. The overall system architecture is presented in Fig. 2.

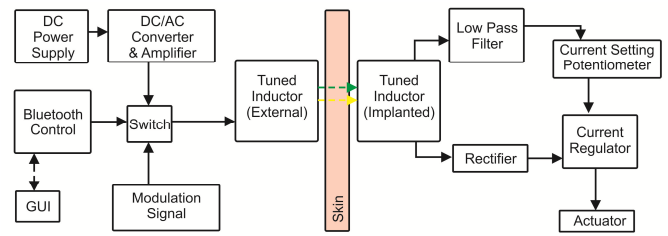


Figure 2: System architecture of ASK modulation circuit to enable wireless flow control.

C. Circuit Design and Layout

a) Transmitter

A 2MHz clock oscillator (ECS -2100, ECS international, Olathe, KS) was used to create the power signal. A quad bilateral switch (CD4016BC, Fairchild Semiconductor, San Jose CA) controlled by the Easy Bluetooth module and Basic Stamp microcontroller kit (Parallax Inc., Rocklin, CA) switched between the power signal or the modulation signal. The generated signal was then amplified in two stages before being applied to a tuned transmitting coil (8 turns of 20 AWG single strand wire, size: 310 mm x 140 mm).

b) Receiver

Litz wire (6 turns, 50/54 SPN/SN Litz Wire, Wiretron, Volcano, CA) was used for the receiving coil ($\varnothing 22$ mm). The circuit components (including the current regulator) require a direct current (DC) power signal. Therefore, the received alternating signal was fully rectified using two Schottky diodes (BAT54A and BAT54C, Fairchild Semiconductor, San Jose, CA). The modulation signal was separated by half-wave rectification (BAT54A) and then filtered using a low pass RC design. Two zener voltage regulator diodes (BZV55, NXP Semiconductors, Eindhoven, Netherlands) regulate the output voltage of the power and demodulated signal. AD5227 (Analog Devices, Norwood, MA) was used as the current setting potentiometer to set the output current of the current regulator (PSSI2021SAY, NXP Semiconductors, Eindhoven, Netherlands). A low frequency

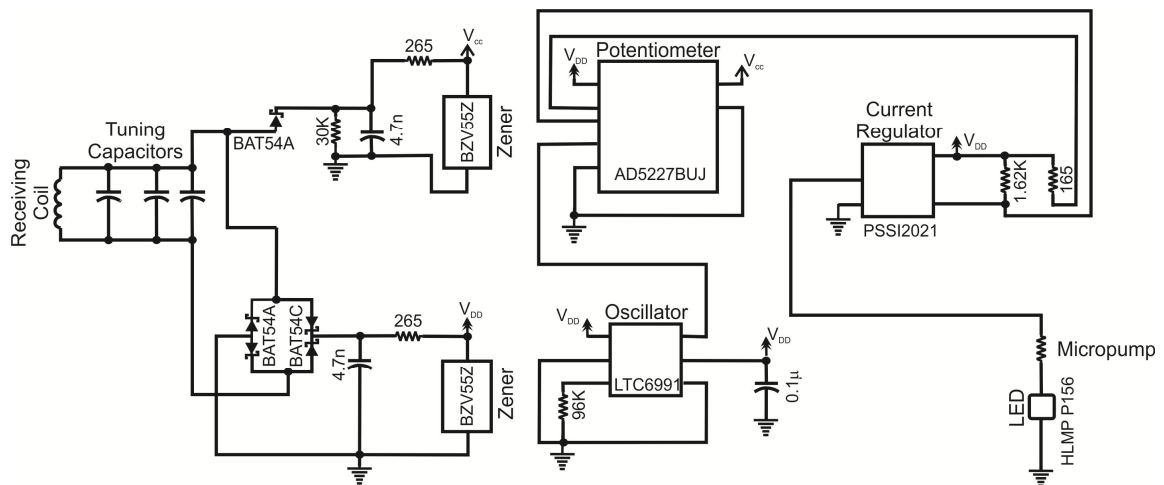


Figure 3: Schematic diagram of the receiver circuit.

oscillator (LTC 6991, Linear Technology, Milpitas, CA) set the potentiometer frequency to 500 Hz. An LED was added in series with the infusion pump to provide visual confirmation of power supply to the actuator (Fig. 3). The receiver was implemented on a flexible printed circuit board (PCB) to allow it to be wrapped around the round micropump. Small surface mount components were chosen to minimize the overall circuit footprint (Fig. 4).

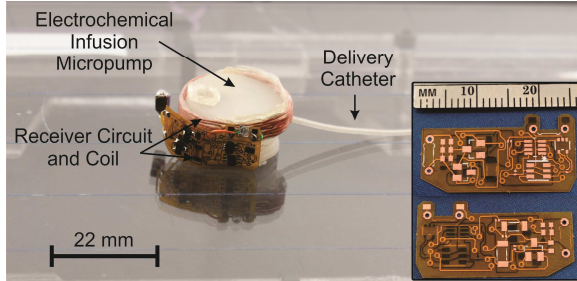


Figure 4: Micropump with integrated receiver. Inset: Receiver flexible PCB, front and back.

III. EXPERIMENTAL METHODS

The transmitter and receiver circuits were first tested using discrete components on breadboards and then on PCBs. Preliminary benchtop testing using a “dummy” 1 k Ω load in place of an actuator was performed to ensure feasibility and repeatability of the approach. The circuit performance was then tested with a micropump on benchtop. In order to study the electric and magnetic effects of tissue on the wireless transmission, testing across simulated brain tissue material [20] was performed.

A. Testing with “Dummy” Load

The receiver current output was increased incrementally (10 steps) and the values achieved were compared to theoretical values calculated based on equations provided in the potentiometer and current regulator datasheets. The output current was calculated by measuring the voltage across a 1 k Ω load. Repeatability of the output current for a specific modulation program was also tested by varying the current in 4 steps: 0.6, 2.6, 0.7, and 2 mA applied successively for each run ($n=5$).

B. Testing with Infusion Pump

An infusion pump with a 1 mL reservoir [15] was connected to the receiver circuit (Fig. 4). Two different regimens were selected to demonstrate wireless operation at multiple flow rates. First, the current output was increased in 0.5 mA steps from 0.6 - 2.1 mA. For the second regimen, the current was increased from 0.6 to 1.2 mA, then decreased to 0.6 mA and increased to 2.2 mA. For both experiments, double distilled (DD) water was used as the drug model, and the infusion flow rate was calculated by measuring the fluid front movement in a calibrated 100 μ L micropipette connected to the outlet of the pump.

C. Testing in Simulated Brain Tissue Material

In order to mimic the effects of wireless transmission through tissue, brain tissue was simulated according to the recipe described in [20]. Briefly, sugar, NaCl salt, and Natrosol[®] (hydroxyethylcellulose, Ashland Inc., Covington, KY) were dissolved in 800 mL of DD water (1108.9, 49.5,

and 19.8 g, respectively). 1.98 g of ProClin[®] 950 preservative (Sigma-Aldrich, St. Louis, MO) was added as a replacement for Dowcicl 75[®] (1-(3-chloroallyl)-3, 5, 7-triazalazoniaadamantanechloride). A 4 cm thick slab of gel-like material was created for testing. The pump and circuit were then placed on top of the simulated brain tissue. Different current values were applied using the Basic Stamp editor program and the infusion flow rate was calculated by measuring the fluid front movement in a calibrated 100 μ L micropipette. The simulated tissue material was then removed and the experiment repeated with only air separating the transmitter and receiver.

IV. RESULTS & DISCUSSION

A. Testing with “Dummy” Load

The results for the incremental increase in receiver current output are shown in Fig. 5. The measured value closely followed the expected value for all the modification steps. Repeatability in achieved current output for the same modulation program was also confirmed (Fig. 6).

B. Testing with Infusion Pump

Fig. 7 shows the variable current results with the infusion pump. The measured flow rate closely followed the changes in current initiated using the interface program. Measured flow rate values were comparable to those achieved for wired actuation of the infusion pump [15].

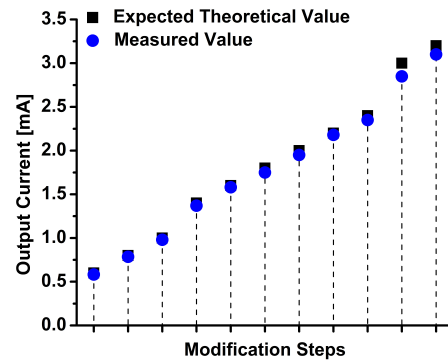


Figure 5: 10 step incremental increase in receiver current output measured across a 1 k Ω resistor (at each modification step, a specific pulse width was applied to achieve the desired change in the wiper position; the values were calculated based on equations provided in the potentiometer and current regulator datasheets)

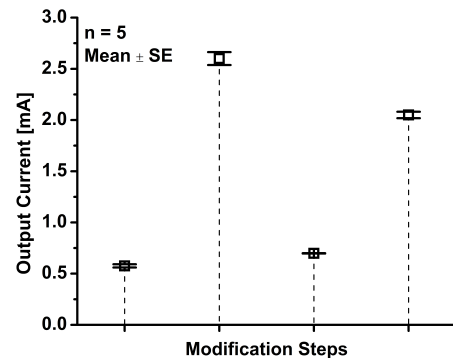


Figure 6: Current output repeatability for a specific modulation program.

C. Testing in Simulated Brain Tissue Material

Successful current modulation was achieved through the simulated brain tissue material (data not shown; no significant difference was observed between infusion flow rates for wireless transmission through air vs. simulated tissue; one way analysis of variance, $p < 0.05$). However, in both cases, the achieved flow rate was smaller than that observed for when the pump was placed directly above the transmitter coil (15% decrease). As previously mentioned, flow rate is linearly dependent on applied current, and therefore, dependent on received power. As a result, decreased power transfer due to coil distance leads to decreased flow rate. The decrease in power transfer with distance between the coils can be mitigated by increasing the power output of the transmitter [13].

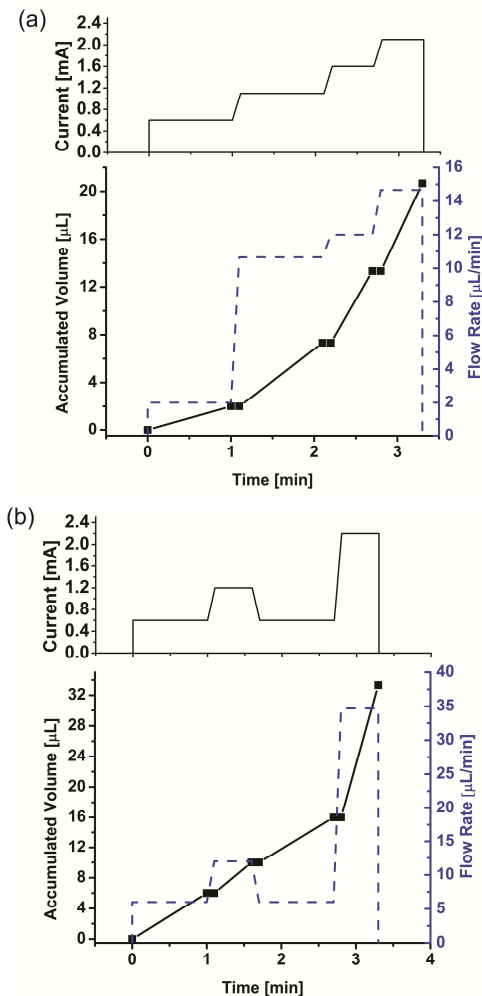


Figure 7: Wireless flow variation in (a) incremental steps, and (b) random fashion.

V. CONCLUSION

A completely wireless infusion micropump system with flow rate adjustability (2.0 – 25.0 $\mu\text{L}/\text{min}$ for 0.6-3.2 mA applied current) capable of achieving patient-tailored therapy was presented. A decrease in power transmission was observed when transmitter and receiver coil distance and angle foveation were increased. This resulted in a flow rate decrease. Performance can be improved if necessary by

increasing the power transmitted and inclusion of a second receiver coil. Future work includes integration with an electrochemically based dose tracking system capable of real-time tracking, confirmation of delivery [21].

ACKNOWLEDGMENT

The authors thank Dr. C. A. Gutierrez and the members of the USC Biomedical Microsystems Laboratory for their assistance.

REFERENCES

- [1] K. Menehan, "Partnership for Solutions: Better Lives for People with Chronic Conditions," Robert Wood Johnson Foundation, 2006.
- [2] Centers for Disease Control and Prevention. (2014, *Chronic Disease Prevention and Health Promotion*. Available: <http://www.cdc.gov/chronicdisease/>
- [3] J. Urquhart, et. al., "Rate-controlled delivery systems in drug and hormone research," *Ann. rev. of pharm. and tox.*, vol. 24, pp. 199-236, 1984.
- [4] J. Fiering, et. al., "Local drug delivery with a self-contained, programmable, microfluidic system," *Biomed. Microdev.*, vol. 11, pp. 571-578, 2009.
- [5] B. Bruguerolle and G. Labrecque, "Rhythmic pattern in pain and their chronotherapy," *Ad. Drug Del. Rev.*, vol. 59, pp. 883-895, 2007.
- [6] B.-B. C. Youan, "Chronopharmaceutics: Gimmick or clinically relevant approach to drug delivery?," *J. of Cont. Rel.*, vol. 98, pp. 337-353, 2004.
- [7] W. Hrushesky, "Cancer chronotherapy: A drug delivery challenge," *Prog. in Clinical and Biological Res. A*, vol. 341, pp. 1-10, 1990.
- [8] F. Halberg, et. al., "Toward a chronotherapy of neoplasia: tolerance of treatment depends upon host rhythms," *Cell. and Mol. Life Sci.*, vol. 29, pp. 909-934, 1973.
- [9] C. G. Lis, et. al., "Circadian timing in cancer treatment: the biological foundation for an integrative approach," *Integrative cancer therapies*, vol. 2, pp. 105-111, 2003.
- [10] E. Meng and T. Hoang, "MEMS-enabled implantable drug infusion pumps for laboratory animal research, preclinical, and clinical applications," *Ad. Drug Del. Rev.*, 2012.
- [11] D. Paolino, et. al., "Drug delivery systems," *Enc. of Med. Devices and Inst.*, 2006.
- [12] D. J. H. Tng, et. al., "Approaches and Challenges of Engineering Implantable Microelectromechanical Systems (MEMS) Drug Delivery Systems for in Vitro and in Vivo Applications," *Micromachines*, vol. 3, pp. 615-631, 2012.
- [13] R. Sheybani, et. al., "Drug Delivery Using Wireless MEMS," in *Handbook of MEMS for wireless and mobile applications*, Uttamchandani, Ed., ed: Woodhead Pub., 2013, pp. 489-517.
- [14] P. Si, et. al., "Wireless power supply for implantable biomedical device based on primary input voltage regulation," in *ICIECA 2007*, pp. 235-9.
- [15] R. Sheybani, et. al., "A MEMS electrochemical bellows actuator for fluid metering applications," *Biomed. Microdev.*, pp. 1-12, 2012.
- [16] R. Sheybani and E. Meng, "Electrochemical Drug Infusion Micropump with Wide Dynamic Range and Viscosity Independent Pumping," in *BMES 2012*.
- [17] J. Xie, et. al., "An Electrochemical Pumping System for On-Chip Gradient Generation," *Anal. Chem.*, vol. 76, pp. 3756-3763, 2004.
- [18] S. Shibata, "Supersaturation of oxygen in acidic solution in the vicinity of an oxygen-evolving platinum anode," *Electrochimica Acta*, vol. 23, pp. 619-623, 1978.
- [19] C. W. M. P. Sillen, et. al., "Gas bubble behaviour during water electrolysis," *Int. J. of Hydrogen Energy*, vol. 7, pp. 577-87, 1982.
- [20] G. Hartsgrrove, et. al., "Simulated biological materials for electromagnetic radiation absorption studies," *Bioelectromagnetics*, vol. 8, pp. 29-36, 1987.
- [21] R. Sheybani, et. al., "Design, fabrication, and characterization of an electrochemically-based dose tracking system for closed-loop drug delivery," *EMBC 2012*, pp. 519-522.